Response of Functionally Graded Material Plate under Constant Thermal Loading

Anju M[1] Dr Subha K[2]
[1]PG Student [2]Professor
[1,2]Department of Civil Engineering
[1,2]NSSCE Palakkad, Kerala, India

Abstract— Functionally graded material comes under the classification of composite material that have a continuous variation of material properties along the thickness direction. The overall properties of FGM can be varied according to our needs, thus one of the main advantages of such a material is that it can be tailored specifically for serving a particular function that makes it unique from any of the base materials used in its synthesis. In the present project, a study on the thermal behavior of metal-ceramic FGM plate is conducted under constant thermal loading. The results thus obtained are compared with other standard results and thus validated. The material properties are varied using different homogenization schemes and the results are compared.

Key words: Functionally Graded Materials, Material Properties, Thermal Behaviour, Thermal Loading, Homogenisation Schemes

I. INTRODUCTION

While laminated composite materials provide the design flexibility to achieve desirable stiffness and strength through the choice of lamination scheme, the anisotropic constitution of laminated composite structures often results in stress concentrations near material and geometric discontinuities that can lead to damage in the form of delamination, matrix cracking, and adhesive bond separation. Functionally gradient materials (FGM) are a class of composites that have a continuous variation of material properties from one surface to another and thus alleviate the stress concentrations found in laminated composites. The gradation in properties of the material reduces thermal stresses, residual stresses, and stress concentration factors. The gradual variation results in a very efficient material tailored to suit the needs of the structure and therefore is called a functionally graded material. They are typically manufactured from isotropic components such as metals and ceramics since they are mainly used as thermal barrier structures in environments with severe thermal gradients (e.g., thermoelectric devices for energy conversion, semiconductor industry). In such applications the ceramic provides heat and corrosion resistance; meanwhile the metal provides the strength and toughness. Thin-walled members, i.e., plates and shells, used in reactor vessels, turbines and other machine parts are susceptible to failure from buckling, large amplitude deflections, or excessive stresses induced by thermal or combined thermo-mechanical loading. The main applications of functionally gradient materials have been in high temperature environments, including thermal shock - a situation that arises when a body is subjected to a high transient heating or cooling in a short time period.

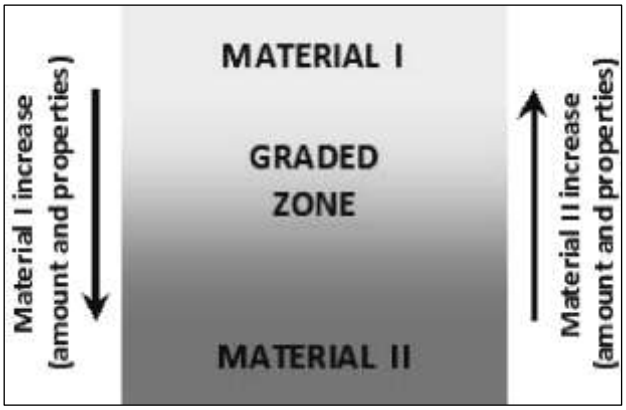

Fig. 1: Schematic diagram of continuously graded FGM

A. Applications

The FGM concept is applicable to almost all material fields. Potential applications include those structural and engineering uses that require combinations of incompatible functions such as refractoriness or hardness with toughness, or chemical inertness with toughness. In aerospace and nuclear energy applications, reliability rather than cost is the key issue. But in applications such as cutting tools, high temperature rollers, and engine components, which require wear, heat, mechanical shock, and corrosion resistance; the key issues are the cost/performance ratio and reliability. Two applications now commercialized are high performance cutting tools of tungsten carbide/cobalt based FGMs and razor blades of an iron aluminide/stainless steel FGM. The successful FGM applications for cutting tools and biomaterials have in common that their graded structures are formed in situ, and their relatively small size makes it feasible to process them cost effectively. To protect the environment and conserve nonrenewable energy resources, energy conversion systems that do not produce atmospheric pollutants such as thermionic and thermoelectric converters, fuel cells, and solar batteries are under active development. The incorporation of the concept into their total FGM design can improve their conversion efficiency by optimizing their electronic potential, thermal stress resistance, and chemical durability. Although the practical applications of FGMs have not yet been fully realized and exploited, it is the belief that the impact of the FGM concept itself, which can potentially impact almost all materials research and development, will begin to emerge in the 21st century.

II. CHARACTERIZATION OF PROPERTIES

The technology of Functionally Graded Materials (FGMs) enables the realization of innovative and multiple functions that cannot be achieved with conventional homogeneous materials. Predetermined chemical composition profiles (the spatial distribution of their components) as well as

predetermined transitions in their microstructure, are intentionally introduced to perform desired functions. Therefore, in order to use FGMs in practical applications, it is important to characterize their properties. The characterization of properties includes evaluating the local microstructure and properties of the FGM to determine the potential performance of the designed structure and the distribution of its properties. It also includes the evaluation of the overall performance of the material's properties. In the microstructural evaluation, it is necessary to quantitatively determine the size, configuration, orientation, and contiguity of phases. This can be accomplished using ordinary image analysis. In some cases, conventional techniques can be used such as micro scale chemical analysis and micro hardness tests. But in others, some modifications in the techniques are necessary because the continuous change in the properties in a local region make measurement difficult. However, in evaluating the overall performance of properties such as electrical, magnetic, thermal, and mechanical, if conventional methods are not applicable, it may be necessary to modify them or even to develop new techniques. Furthermore, fracture behavior in a ceramic/metal FGM can change from brittle to ductile fracture due to the gradual change in the contiguity of the ductile, metal phase. Consequently, the overall mechanical behavior of an FGM has to be evaluated not only on the macroscopic scale but also on the microscopic scale, such as for damage growth, micro crack initiation at interfaces, and crack propagation. The evaluation of thermal stress is also important, because thermal stresses are generated during an FGM's fabrication and heat treatment as well as by differences in the coefficients of thermal expansion (CTE) of its components.

A. Homogenization scheme

1) Voigt Scheme:

Voigt model has been adopted in most analyses of FGM structures. The advantage of Voigt method is that it is easy to calculate and can be considered as the upper and lower bounds for the effective elastic properties of a heterogeneous material. The effective material properties P_f, like Young's modulus E_f, Poisson' ratio ν_f, thermal expansion coefficient α_f, and thermal conductivity K_f may be expressed as,

$$P_f = P_t \times V_C + P_b \times V_m$$

Where, P_t and P_b denoted the temperature-dependent properties of the top and bottom surfaces of the plate, respectively. Vm and Vc and are the metal and ceramic volume fractions which can be expressed by

$$V_C + V_m = 1$$

If volume fraction Vc is assumed to follow a simple power law as

$$V_C = \left(\frac{z}{h} + 0.5\right)^n$$

Where, 'n' is the volume fraction index and takes only positive values

$$E_z = E_1 + (E_C - E_m)\, V_C$$
$$\alpha_z = \alpha_m + (\alpha_c - \alpha_m) V_C$$
$$k_z = k_m + (k_c - k_m) V_C$$

2) Mori-Tanaka Scheme:

Mori and Tanaka formulated a method to calculate the average internal stress in the matrix of a material which has been again reformulated by Benveniste for the application in composite materials. Such method works well for composites with discontinuous particle phase regions of graded microstructure. The volume fraction is assumed to follow a simple power law. According to this scheme, effective Bulk and shear modulus are given by the relation

$$K_e = K_b + \frac{Vc \times K_{diff}}{1 + \frac{V_m \times K_{diff}}{K_b + 1.33\mu_b}}$$
$$\mu_e = \mu_b + \frac{V_C \times K_{diff}}{1 + \frac{K_m \times K_{diff}}{K_b + f_1}}$$

Where,

$$K_{diff} = K_t - K_b$$
$$\mu_{diff} = \mu_t - \mu_b$$
$$f_1 = \mu_b \times \frac{9K_b + 8\mu_b}{6(K_b + 2\mu_b)}$$

Young's modulus (E), Poisson's ratio (υ) can be calculated from them as given below.

$$E = \frac{9K_e \times \mu_e}{3K_e + \mu_e}$$
$$\mu = \frac{3K_e - 2\mu_e}{2 \times (3K_e + \mu_e)}$$

3) Sigmoid Function:

The use of power law distribution results in sharp gradients in material properties when the power law index moves away from unity. Smooth distribution of properties can be ensured by using two power law functions to describe the distribution. Therefore, to ensure smooth distribution of stresses among all the interfaces, Chung and Chi (2001) defined the volume fraction using two power-law functions. The two power law functions are defined by

$$f_1(z) = 1 - \frac{1}{2}\left[1 - \frac{2z}{h}\right]^p \quad \text{for } 0 \le z \le \frac{h}{2} \text{ and}$$
$$f_2(z) = \frac{1}{2}\left[1 - \frac{2z}{h}\right]^p \quad \text{for } 0 \le z \le \frac{h}{2}$$

By using rule of mixtures, the young's modulus of the FGM can be written as,

$$E(Z) = f_1(z) \times E_1 + \left(1 - f_1(z)\right) \times E_2 \text{ for } 0 \le z \le \frac{h}{2}$$
$$E(Z) = f_2(z) \times E_1 + \left(1 - f_2(z)\right) \times E_2 \text{ for } -\frac{h}{2} \le z \le 0$$

4) Exponential Function:

This law is generally adopted by the researches when they deal with the fracture mechanics problems. According to this law the material property in P(z) in a specific direction is given by,

$$P(z) = P_t e^{\left(\frac{1}{h}\right)\left(\ln\frac{P_b}{P_t}\right)\left(z + \frac{h}{2}\right)}$$

III. VALIDATION

A validation study has been conducted for deformation values from the available literature. A work by Manoj Sharma et al. 'Deflection of Functionally Graded Material Plate under Mechanical Thermal and Thermo-Mechanical Loading' is identified for this purpose. The specific system investigated is Aluminum-Zirconia. The FGM modelling is done one side of the material as ceramic and the other side as metal. Table 1 shows the values of all the material properties used in this work.

Sl. No	Property	Aluminum	Zirconia
1	Young's modulus	70GPa	151GPa
2	Poisson's ratio	0.3	0.3
3	Thermal conductivity	204W/Mk	2.09W/mK
4	Thermal expansion	23e-6 / ° C	10e-6 / ° C

Table 1: Material properties

The static analysis was performed on a square plate of side length a = b = 0.2m and thickness h=0.01m. The plate is assumed to be simply supported on all its edges. A regular 8 by 8 mesh of linear elements in a full size plate was chosen. The value of the uniformly distributed loading was equal to $q_o = 0.01 \times 10^6$ N/m^2 and the plate is subjected to a temperature field where the uniform temperature up to 300 °C is given and the reference surface temperature is held at 20 °C. The materials are assumed to be perfectly elastic throughout the deformation. The analysis was performed for fix values of the volume fraction exponent n = 2.

Distance along X direction (m)	Deformation m	
	Manoj Sharma et al. (2013)	Present work
0	0.160e-5	0.159e-5
0.014	0.240e-5	0.238e-5
0.028	0.321e-5	0.318e-5
0.042	0.401e-5	0.397e-5
0.056	0.482e-5	0.477e-5
0.070	0.561e-5	0.556e-5
.084	0.641e-5	0.635e-5
0.1	0.721e-5	0.715e-5

Table 2: variation of deformation for mechanical loading for n=2

Distance along X direction (m)	Deformation (m)	
	Manoj sharma et al. (2013)	Present work
0	0.000423	0.000421
0.014	0.000634	0.000605
0.028	0.000845	0.000789
0.042	0.001056	0.000972
0.056	0.001268	0.001156
0.070	0.001479	0.001340
0.084	0.001690	0.001524
0.1	0.1902	0.1708

Table-3: variation of deformation for thermo-mechanical loading for n=2

The results obtained are comparable.

IV. NUMERICAL ANALYSIS

Numerical results are presented for ceramic-metal FGM plates. The metal is taken to be aluminum and the ceramic used is alumina. The properties for the two materials are listed below.

Sl. No	property	aluminum	zirconia
1	Young's modulus	70GPa	151GPa
2	Poisson's ratio	0.3	0.3
3	Thermal conductivity	204W/Mk	2.09W/mK
4	Thermal expansion	23e-6 / ° C	10e-6 / ° C

Table 4: Material properties

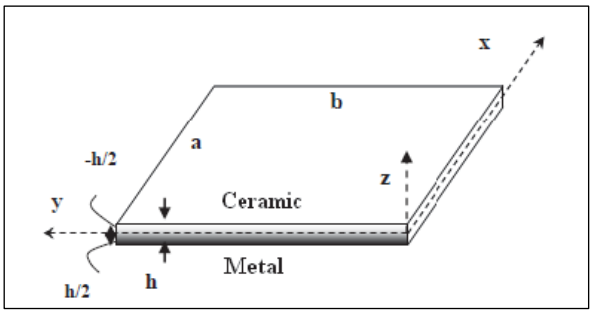

Fig. 2: Plate geometry

The boundary conditions considered are all sides simply supported. Because of the biaxial symmetry of the problem, the computational domain is taken to be the positive quadrant. A regular mesh of 10 x 10 is used. The plate is modelled using the shell element 181 in ANSYS APDL 17.0. It is a four node element with six degrees of freedom at each node: translations in the x, y, and z directions, and rotations about the x, y, and z-axes. It can be used to model thin to moderately thick shells. It comes under the first order shear deformation theory.

The metal surface is exposed to 20°C and the ceramic surface is exposed to fixed but different temperatures. The melting point of aluminum alloy 2219 is 543°C and that of alumina is 2040°C. Thus, using 0 to 500°C for aluminum plate is not realistic (the modulus and other properties of aluminum will change long before its temperature reaches 600°C), but the purpose is to establish the bounds for the FGM analysis. The power index values varies from 0 to ∞. ie when n=0 the plate is fully ceramic and when n=∞, the plate is fully metal.

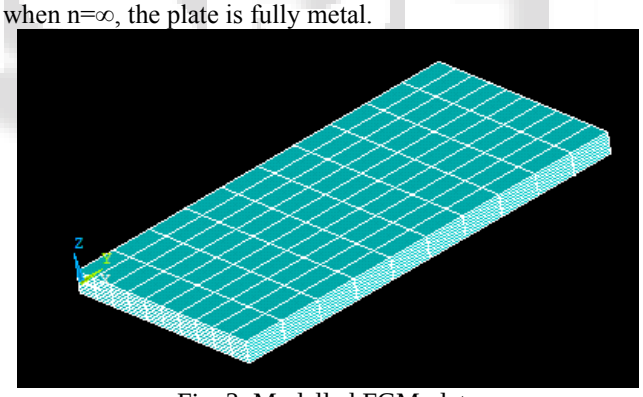

Fig. 3: Modelled FGM plate

A. Tensile stress

The values obtained tensile stress for FGM plate by applying different thermal loads are given below

1) Voigt scheme:

Power index n	a/b=0.5 a/h=10				
	Tensile Stress (y direction) (N/m^2)				
	300 °C	350 °C	400 °C	450 °C	500 °C
0	8.67E +8	1.02E +9	1.18E +9	1.33E +9	1.49E +9
0.5	9.22E +8	1.09E +9	1.25E +9	1.42E +9	1.58E +9
1	9.07E +8	1.07E +9	1.23E +9	1.39E +9	1.55E +9
2	8.63E +8	1.02E +9	1.17E +9	1.33E +9	1.48E +9

5	7.98E +8	9.40E +8	1.08E +9	1.23E +9	1.37E +9
10	7.64E +8	9.00E +8	1.04E +9	1.17E +9	1.31E +9
50	7.74E +8	9.12E +8	1.05E +9	1.19E +9	1.33E +9
∞	4.57E +8	5.39E +8	6.20E +8	7.02E +8	7.84E +8

Table 5: Tensile stress for different thickness ratio under constant thermal loads for a//b=0.5 a/h=10

It can be seen that under all the constant thermal loads the variation of tensile stress is the same.

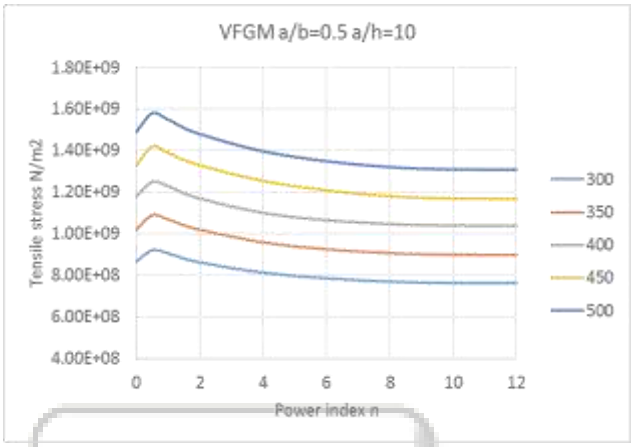

Chart 1: Variation of tensile stress with respect to constant thermal loads for different 'n' values for Voigt Scheme for a/h=10.

a/b=0.5 a/h=5					
Power index n	Tensile Stress (y direction) (N/m^2)				
	300 °C	350 °C	400 °C	450 °C	500 °C
0	8.67E +8	1.02E +9	1.18E +9	1.33E +9	1.49E +9
0.5	9.15E +8	1.08E +9	1.24E +9	1.41E +9	1.57E +9
1	8.92E +8	1.05E +9	1.21E +9	1.37E +9	1.53E +9
2	8.36E +8	9.85E +8	1.13E +9	1.28E +9	1.43E +9
5	7.54E +8	8.88E +8	1.02E +9	1.16E +9	1.29E +9
10	7.32E +8	8.62E +8	9.93E +8	1.12E +9	1.25E +9
50	7.52E +8	8.86E +8	1.02E +9	1.15E +9	1.29E +9
∞	4.57E +8	5.39E +8	6.20E +8	7.02E +8	7.84E +8

Table 6: Tensile stress for different thickness ratio under constant thermal loads for a//b=0.5 a/h=5

When comparing with the results of thickness ratios a/h=10, the values of tensile stress for a/h=5 is smaller.

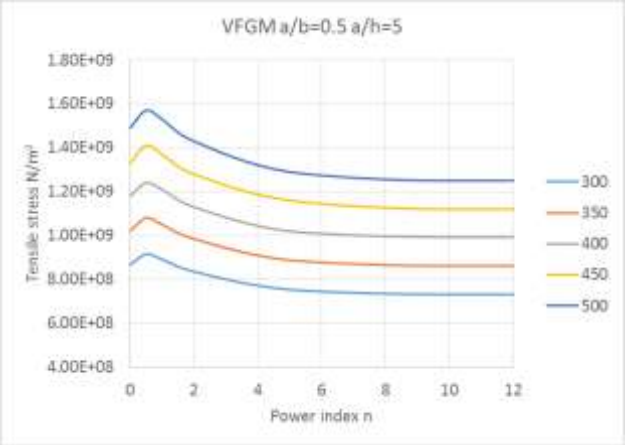

Chart 2: Variation of tensile stress with respect to constant thermal loads for different 'n' values for Voigt Scheme for a/b=0.5 a/h=5.

2) Mori Tanaka scheme:

a/b=0.5 a/h=10					
Power index n	Tensile stress (x/y direction) N/m^2				
	300 °C	350 °C	400 °C	450 °C	500 °C
0	8.03E +8	9.53E +8	1.10E +9	1.24E +9	1.39E +9
0.5	8.82E +8	1.04E +9	1.20E +9	1.35E +9	1.51E +9
1	8.41E +8	9.91E +8	1.14E +9	1.29E +9	1.44E +9
2	7.98E +8	9.40E +8	1.08E +9	1.23E +9	1.37E +9
5	7.70E +8	9.07E +8	1.04E +9	1.18E +9	1.32E +9
10	7.70E +8	9.08E +8	1.05E +9	1.18E +9	1.32E +9
50	7.76E +8	9.15E +8	1.05E +9	1.19E +9	1.33E +9
∞	4.26E +8	5.02E +8	5.78E +8	6.55E +8	7.31E +8

Table 3: Tensile stress for different thickness ratio under constant thermal loads for a/b=1 a/h=10

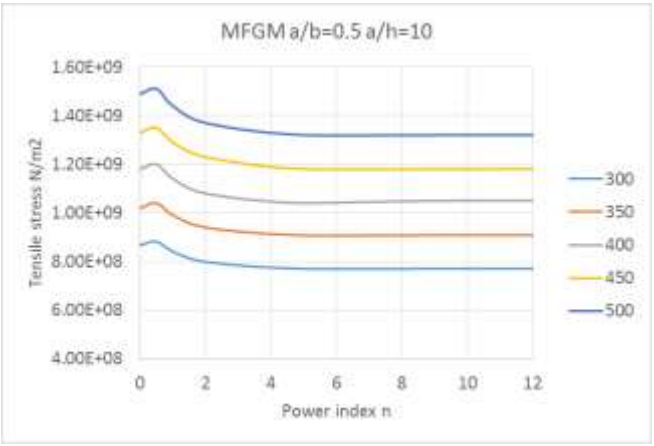

Chart 3: Variation of tensile stress with respect to constant thermal loads for different 'n' Values for Mori Tanaka Scheme for a/b=0.5 a/h=10

a/b=0.5 a/b=5					
Power index n	Tensile stress (x/y direction) N/m^2				
	300 °C	350 °C	400 °C	450 °C	500 °C

0	8.08E+8	9.53E+8	1.10E+9	1.24E+9	1.39E+9
0.5	8.68E+8	1.03E+9	1.21E+9	1.38E+9	1.54E+9
1	8.15E+8	9.60E+8	1.11E+9	1.25E+9	1.40E+9
2	7.66E+8	9.03E+8	1.04E+9	1.8E+09	1.31E+9
5	7.50E+8	8.84E+8	1.02E+9	1.15E+9	1.29E+9
10	7.44E+8	8.76E+8	1.01E+9	1.14E+9	1.27E+9
50	7.53E+8	8.87E+8	1.02E+9	1.16E+9	1.29E+9
∞	4.26E+8	5.02E+8	5.78E+8	6.55E+8	7.31E+8

Table 4: Tensile stress for different thickness ratio under constant thermal loads for a/b=1 a/h=5 of Mori-Tanaka scheme

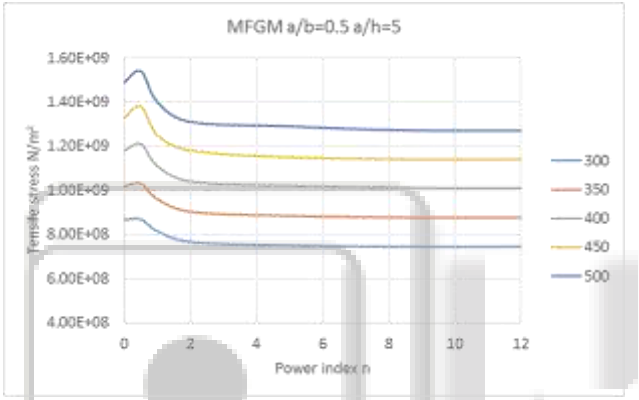

Chart 4: Variation of tensile stress with respect to constant thermal loads for different 'n' Values for Mori Tanaka Scheme for a/b=0.5 a/h=5

When the power index value exceeds 2, the tensile stress tends to a constant value.

3) Sigmoidal scheme:

a/b=0.5 a/h=10					
Power index n	Tensile stress (y direction) N/m²				
	300 °C	350 °C	400 °C	450 °C	500 °C
0	8.67E+8	1.02E+9	1.18E+9	1.33E+9	1.49E+09
0.5	8.62E+8	1.02E+9	1.17E+9	1.32E+9	1.48E+09
1	9.07E+8	1.07E+9	1.23E+9	1.39E+9	1.55E+09
2	9.50E+8	1.12E+9	1.29E+9	1.46E+9	1.63E+09
5	9.77E+8	1.15E+9	1.33E+9	1.50E+9	1.67E+09
10	9.82E+8	1.16E+9	1.33E+9	1.51E+9	1.68E+09
50	9.83E+8	1.16E+9	1.33E+9	1.51E+9	1.69E+09
∞	4.57E+8	5.39E+8	6.20E+8	7.02E+8	7.84E+08

Table 5: Tensile stress for different thickness ratio under constant thermal loads for a/b=0.5 a/h=10 of sigmoidal scheme

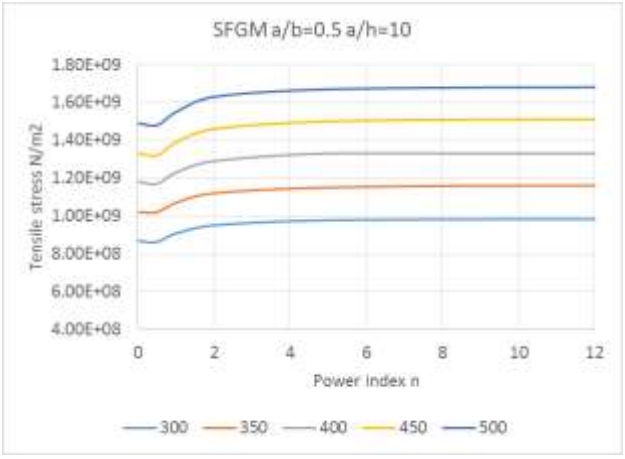

Chart 5: Variation of tensile stress with respect to constant thermal loads for different 'n' Values for Sigmoidal Scheme for a/b=0.5 a/h=10

a/b=0.5 a/h=5					
Power index n	Tensile stress (y direction) N/m²				
	300 °C	350 °C	400 °C	450 °C	500 °C
0	8.67E+8	1.02E+9	1.18E+9	1.33E+9	1.49E+9
0.5	8.50E+8	1.00E+9	1.15E+9	1.31E+9	1.46E+9
1	8.93E+8	1.05E+9	1.21E+9	1.37E+9	1.53E+9
2	9.31E+8	1.10E+9	1.26E+9	1.43E+9	1.60E+9
5	9.54E+8	1.12E+9	1.29E+9	1.47E+9	1.64E+9
10	9.57E+8	1.13E+9	1.30E+9	1.47E+9	1.64E+9
50	9.57E+8	1.13E+9	1.30E+9	1.47E+9	1.64E+9
∞	4.57E+8	5.39E+8	6.20E+8	7.02E+8	7.84E+8

Table 6: Tensile stress for different thickness ratio under constant thermal loads for a/b=0.5 a/h=5 of sigmoidal scheme

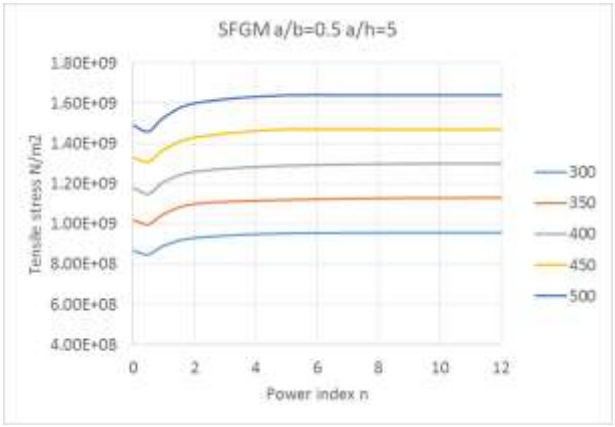

Chart 6: Variation of tensile stress with respect to constant thermal loads for different 'n' Values for Sigmoidal Scheme for a/b=0.5 a/h=5

Unlike the voigt and Mori Tanaka scheme the value of tensile stress for sigmoidal scheme increases with increase in power index value.

4) Exponential scheme:

Since the exponential scheme is independent of the power index value there is only one value for tensile stress for each loading condition.

Aspect ratio a/b=5		
Temperature °C	Tensile stress N/m²	
	a/h=10	a/h=5
300	9.18e8	9.01E+08
350	1.08e9	1.06E+09
400	1.25e9	1.22E+09
450	1.41e9	1.38E+09
500	1.57e9	1.54E+09

Table 7: Tensile stress for different thickness ratio under constant thermal loads for a/b=0.5 of Exponential Scheme

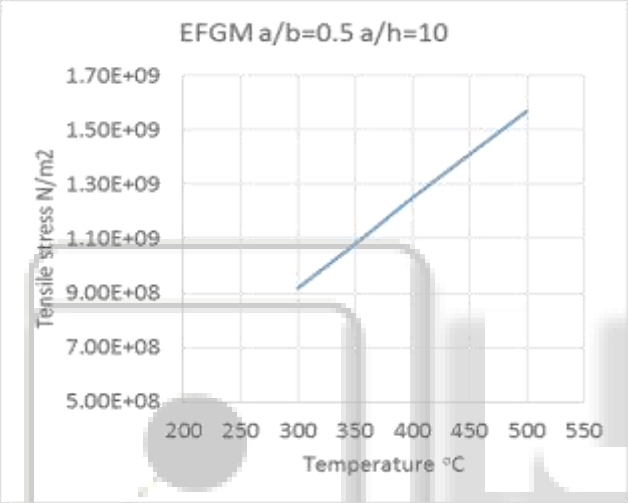

Chart 7: Variation of tensile stress with respect to constant thermal loads for exponential Scheme for a/b=0.5 a/h=5

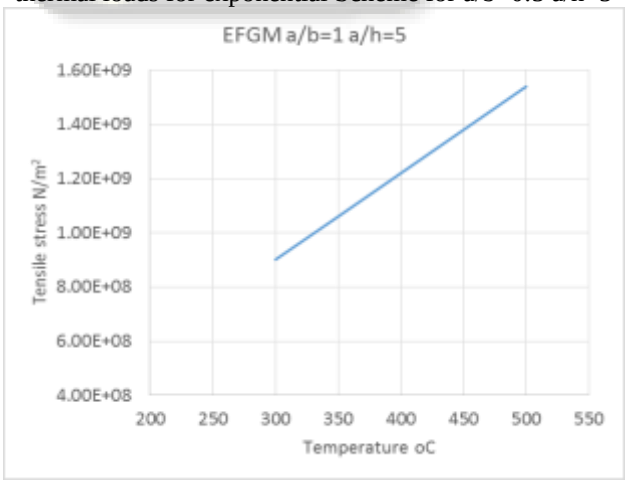

Chart 8: Variation of tensile stress with respect to constant thermal loads for Exponential Scheme for a/b=0.5 a/h=5.

The tensile stress increases with increase in temperature.

B. Deformation

1) Voigt scheme:

a/b=0.5 a/h=10					
Power index n	Deformation m				
	300 °C	350 °C	400 °C	450 °C	500 °C
0	0.00117	0.00138	0.00159	0.00180	0.00201
0.5	0.00140	0.00166	0.00188	0.00217	0.00240
1	0.0018	0.00212	0.00244	0.00276	0.00308
2	0.00199	0.00234	0.00270	0.00305	0.0034
5	0.00219	0.00258	0.00297	0.00336	0.0035
10	0.00185	0.00218	0.00251	0.00284	0.0031
25	0.00187	0.00221	0.00254	0.00290	0.0032
50	0.00189	0.00222	0.00256	0.00290	0.0032
∞	0.00315	0.003712	0.00427	0.00483	0.0054

Table 8: Deformation for different thickness ratio under constant thermal loads for a/b=0.5 a/h=10 of Voigt Scheme

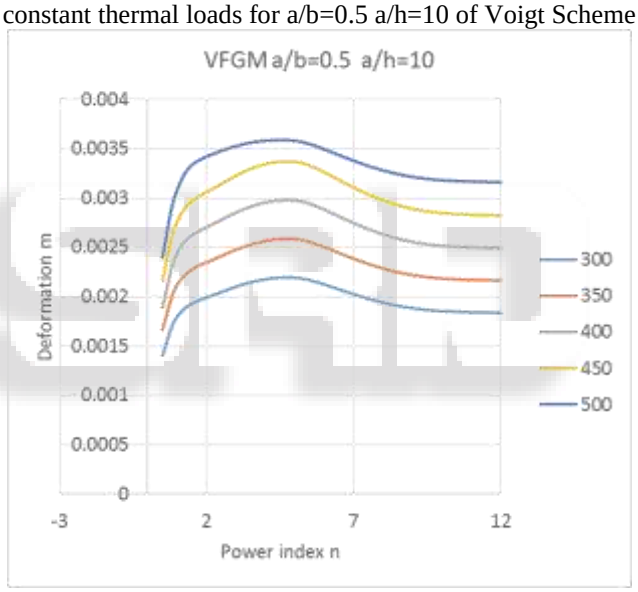

Chart 9: Variation of deformation with respect to constant thermal loads for Voigt Scheme for a/b=0.5 a/h=10

a/b=0.5 a/h=5					
Power index n	Deformation m				
	300 °C	350 °C	400 °C	450 °C	500 °C
0	0.00117	0.00138	0.00159	0.00180	0.002016
0.5	6.94E-4	8.18E-4	9.41E-4	1.07E-3	0.001189
1	8.77E-4	0.00103	1.19E-3	0.00134	1.50E-03
2	9.57E-4	0.00112	0.00129	0.00147	0.001641
5	9.18E-4	0.00108	1.25E-3	0.00140	1.57E-03
10	8.87E-4	0.00104	1.20E-3	0.00136	1.52E-03

25	9.10E-4	0.00107	1.24E-3	0.00139	1.56E-03
50	9.18E-4	0.00108	1.25E-3	0.00141	1.57E-03
∞	0.00315	0.003712	0.00427	0.00483	0.0054

Table 9: Deformation for different thickness ratio under constant thermal loads for a/b=0.5 a/h=5 of Voigt Scheme

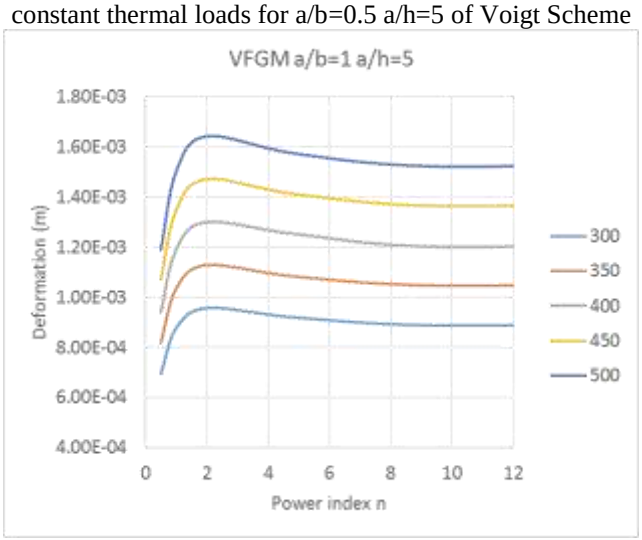

Chart 10: Variation of deformation with respect to constant thermal loads for Voigt Scheme for a/b=0.5 a/h=5.

The values of deformations obtained for FGM plate is less than that obtained for metal plate.

2) Mori Tanaka scheme:

a/b=0.5 a/h=10					
Power index n	Deformation m				
	300 °C	350 °C	400 °C	450 °C	500 °C
0	0.00117	0.00138	0.00159	0.00180	0.00201
0.5	0.00177	0.00209	2.41E-3	0.00272	3.04E-3
1	0.00191	0.00225	2.59E-3	0.00293	3.28E-3
2	0.00191	0.00225	2.60E-3	0.00294	3.29E-3
5	0.00187	0.00221	0.00254	0.00288	0.00321
10	0.00187	0.00221	0.00255	0.00288	0.00322
50	0.00189	0.00223	0.00258	0.00291	0.00326
∞	0.0031	0.003712	0.004275	0.00483	0.00540

Table 10: Deformation for different thickness ratio under constant thermal loads for a/b=0.5 a/h=10 of Mori Tanaka scheme

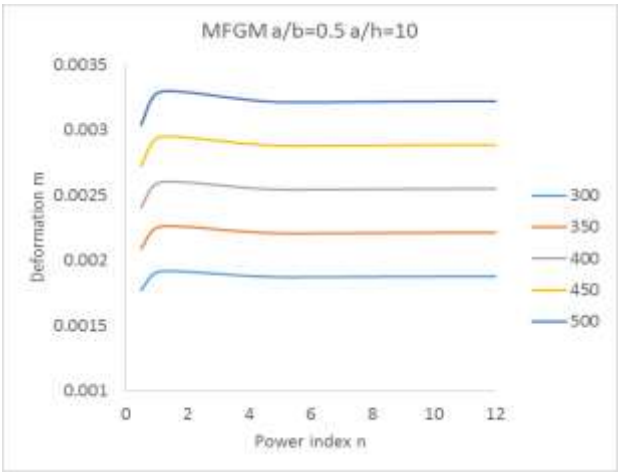

Chart 11: Variation of deformation with respect to constant thermal loads for Mori Tanaka Scheme for a/b=0.5 a/h=10

a/b=0.5 a/h=5					
Power index n	Deformation m				
	300 °C	350 °C	400 °C	450 °C	500 °C
0	0.00117	0.001386	0.001596	0.00180	0.00201
0.5	8.60E-4	0.00101	0.00116	0.00132	0.00147
1	9.19E-4	0.00108	0.00125	0.00141	0.00157
2	9.17E-4	0.00108	0.00124	0.00140	0.00157
5	9.16E-4	0.00108	0.00124	0.00140	0.00157
10	9.07E-4	0.00106	0.00123	0.00139	0.00156
50	9.22E-4	0.00108	0.00125	0.00141	0.00158
∞	0.0031	0.003712	0.00427	0.00483	0.0054

Table 11: Deformation for different thickness ratio under constant thermal loads for a/b=0.5 a/h=5 of Mori Tanaka scheme

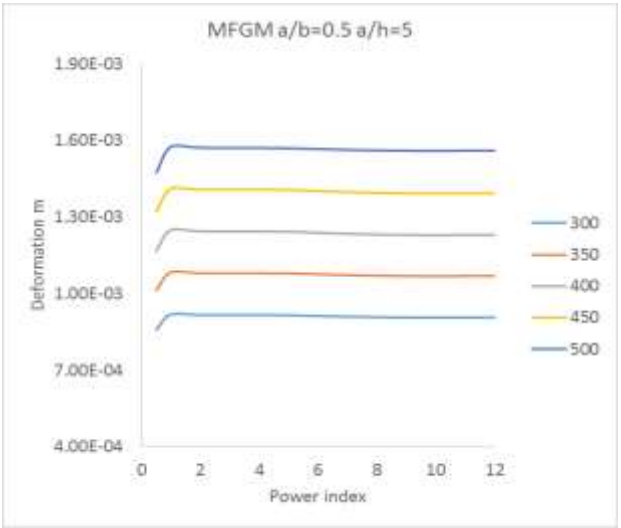

Chart 12: Variation of deformation with respect to constant thermal loads for Mori Tanaka Scheme for a/b=0.5 a/h=5

3) Sigmoidal scheme:

a/b=0.5 a/h=10					
Power index n	Deformation m				
	300 ºC	350 ºC	400 ºC	450 ºC	500 ºC
0	0.00117	0.00138	0.001596	0.00180	0.00201
0.5	0.00150	0.00177	0.002043	0.00231	0.00258
1	0.00180	0.00212	0.00244	0.00276	0.00308
2	0.00202	0.00238	0.002745	0.00310	0.00346
5	0.00204	0.00240	0.00277	0.00313	0.00350
10	0.00198	0.00234	0.00269	0.00304	0.00340
50	0.00195	0.00230	0.00265	0.00300	0.00335
∞	0.00315	0.00371	0.00427	0.00483	0.0054

Table 12: Deformation for different thickness ratio under constant thermal loads for a/b=0.5 a/h=10 of Sigmoidal Scheme

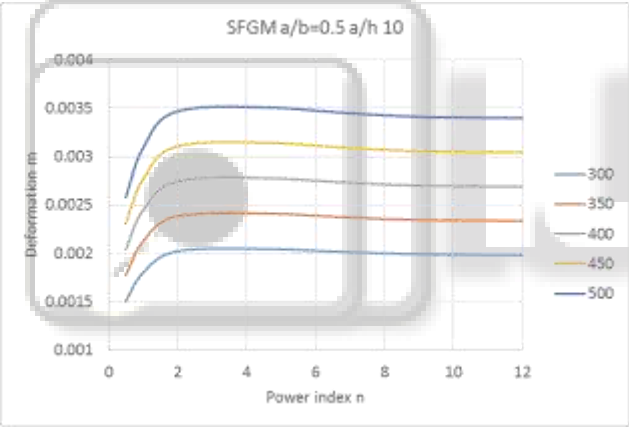

Chart 13: Variation of deformation with respect to constant thermal loads for Sigmoidal Scheme for a/b=0.5 a/h=10.

a/b=0.5 a/h=5					
Power index n	Deformation m				
	300 ºC	350 ºC	400 ºC	450 ºC	500 ºC
0	0.00117	0.00138	0.00159	0.00180	0.00201
0.5	7.34E-4	8.65E-4	9.95E-4	0.00113	0.00125
1	8.77E-4	0.00103	0.00119	0.00134	0.00150
2	9.84E-4	0.00115	0.00133	0.00151	0.00168
5	9.90E-4	0.00116	0.00134	0.00152	0.00169
10	9.59E-4	0.00113	0.00130	0.00147	0.00164
50	9.44E-4	0.00111	0.00128	0.00145	0.00161
∞	0.0031	0.00371	0.00427	0.00483	0.0054

Table 13: Deformation for different thickness ratio under constant thermal loads for a/b=0.5 a/h=5 of Sigmoidal Scheme

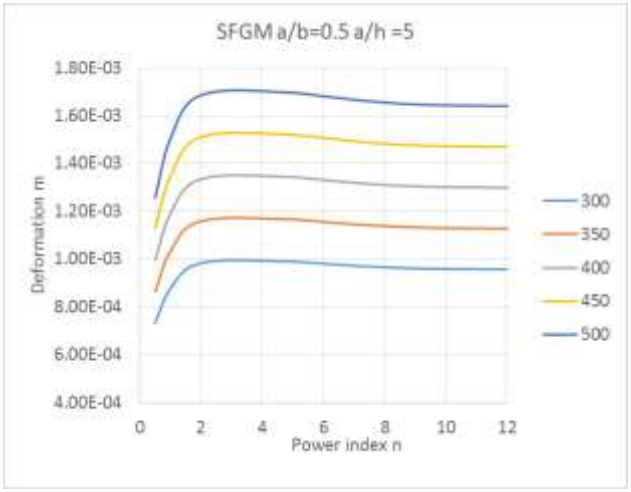

Chart 14: Variation of deformation with respect to constant thermal loads for sigmoidal Scheme for a/b=0.5 a/h=5.

The values of deformations obtained for sigmoidal scheme is higher than the other two schemes.

4) Exponential scheme:

Aspect ratio a/b=0.5		
Temperature ºC	Deformation m	
	a/h=10	a/h=5
300	0.001668	8.07e-4
350	0.001965	9.52e-4
400	0.002263	0.001096
450	0.002561	0.001240
500	0.002859	0.001384

Table 14: Deformation for different thickness ratio under constant thermal loads for a/b=0.5 of Exponential Scheme

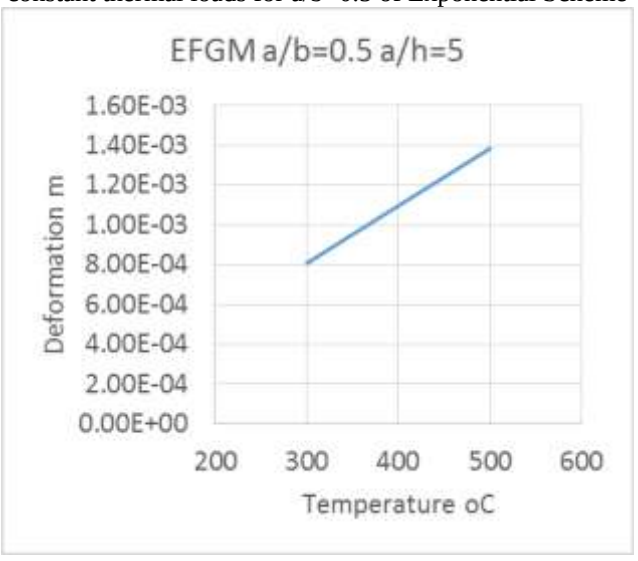

Chart 15: Variation of deformation with respect to constant thermal loads for Exponential Scheme for a/b=0.5 a/h=5

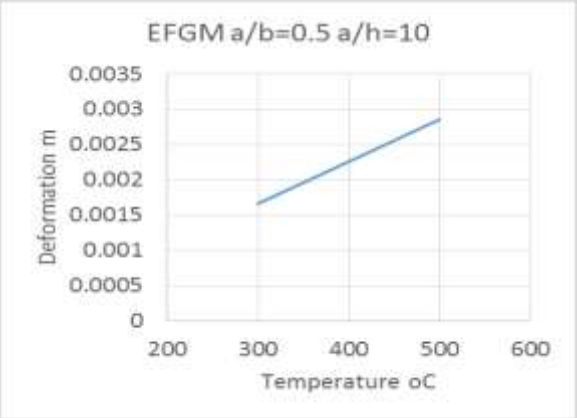

Chart 16: Variation of deformation with respect to constant thermal loads for Exponential Scheme for a/b=0.5 a/h=10

V. CONCLUSION AND FUTURE SCOPE

The following points can be concluded from the conducted studies

1) Among the various homogenization schemes used Exponential function is independent of power exponent 'n' values and hence E-FGM model gives a constant value for both natural frequencies and buckling loads when plotted for different 'n' values.
2) It is observed that the response of plates depends upon the variation of properties from metal to ceramic.
3) Maximum deformation is obtained at the center of the plate and maximum stress at the edges.
4) 4. The results for both deformation and tensile stress calculated using different homogenization schemes tends to increase as the 'a/h' ratio increases as the plate is behaving like thin plates.
5) S-FGM gives the upper-bound results while Mori-Tanaka gives the lower-bound.
6) Stress values decreased with increasing 'n' value as the metallic nature is increasing, that makes the plate more flexible for voigt scheme, mori-tanaka scheme and sigmoidal scheme.
7) The metal plate has the largest deflection here as compared to the other FGM plate and this clearly shows that FGM plate can resist high temperature conditions very well.
8) It is observed that when thermal effect is induced, the bending response of the functionally graded plate is not necessarily intermediate to those of the metal and ceramic plate.
9) In the presence of the above temperature field, compression occurs at the top of the plate and tension is at the bottom surface.
10) The tensile stress depends on the product of the temperature and the thermal expansion coefficient and therefore the response of the graded plate is not intermediate to the metal and ceramic plates.

Some areas for future study includes following points:

1) The present study was conducted for only one boundary condition, i.e. all around simply supported, this can be extended for other boundary conditions also.
2) Only constant temperature field is analyzed here, the analysis can be conducted for other distribution of temperature like linear, nonlinear, polynomial etc.

REFERENCES

[1] Manoj Sharma et al, "Deflection of functionally gradient material plate under mechanical, thermal and thermo-mechanical loading". Global Journal of Researches in Engineering Mechanical & Mechanics, vol.13, 2013, issue 7, pg. 13-18.
[2] K. Swaminathan, "Thermal Analysis of FGM Plates – A Critical Review of Various Modelling Techniques and Solution Methods". Encyclopedia of Thermal Stresses, 2016.
[3] J N Reddy et al, "Thermomechanical analysis of functionally graded cylinders and plates". Journal of Thermal Stresses, 1998, 21, 593-626.
[4] J N Reddy, "Analysis of functionally graded plates". International Journal for Numerical Methods in Engineering, June 1999, 47, 663-684.
[5] Gutierrez-Miravete et al, "Thermal Stresses in Functionally Graded Metal-Ceramic Plates". Excerpt from the Proceedings of the 2015 COMSOL Conference in Boston, 2015.
[6] Bao-Lin Wang et al, "On thermal shock behavior of functionally Graded materials". Journal of Thermal Stresses, 2007, 30, 523-558.
[7] N.Tejaswini et al, "Functionally graded material: an overview". International Journal of Advances in Engineering Science and Technology (IJAEST), 3, 183-188.
[8] Shahistha Aysha et al, "A review on functionally graded materials". The International Journal of Engineering And Science (IJES), 2014, 6, 90-101.
[9] J.R. Cho et al, "Functionally graded material: a parametric study on thermal-stress characteristics using the Crank-Nicolson-Galerkin scheme". Computer Methods in Applied Mechanics and Engineering, 2000 188, 17-38.
[10] Vishesh R Kar, "Effect of temperature on stability behaviour of functionally graded spherical panel". Materials Science and Engineering 2015, 75.
[11] Bhavani V. Sankar et al, (2002), "Thermal Stresses in Functionally Graded Beams". AIAA JOURNAL, 6, 1228-1332.
[12] R. Javaheri et al, "Thermal Buckling of Functionally Graded Plates". AIAA JOURNAL, January 2002, 40, 162-169.
[13] B.A. Samsam Shariat et al, "Thermal buckling of imperfect functionally graded plates". International Journal of Solids and Structures, 2006, 43, 4082-4096.
[14] M. Chmielewski et al, "Metal-ceramic functionally graded materials– manufacturing, characterization, application. Bulletin of the polish academy of sciences Technical sciences, 2016, 1, 151-160.
[15] Senthil S. Vel et al, "Exact Solution for Thermo-elastic Deformations of Functionally Graded Thick Rectangular Plates". AIAA JOURNAL, 2002, 7, 1421-1433.
[16] Mukesh Kumar Saini et al, "Thermal analysis of functionally graded rectangular plate", Third international conference on recent trends in engineering science and management, 2016, 723-735.

